Available online at www.sciencedirect.com
ScienceDirect
International Journal of Pharmaceutics 330 (2007) 121–128
INTERNATIONAL JOURNAL OF PHARMACEUTICS
www.elsevier.com/locate/ijpharm

Oral bioavailability and intestinal secretion of amitriptyline: Role of P-glycoprotein?

Anne-Yvonne Abaut, Francois Chevanne, Pascal Le Corre *

Unité UPRES EA 3892, Laboratoire de Pharmacie Galénique, Biopharmacie et Pharmacie Clinique, Faculté des Sciences Pharmaceutiques et Biologiques, Université de Rennes 1, 2 avenue du Pr Léon Bernard, 35043 Rennes Cedex, France

Received 8 June 2006; received in revised form 31 August 2006; accepted 7 September 2006
Available online 23 September 2006

Abstract

The aim of the study was to evaluate the influence of quinidine, a P-glycoprotein inhibitor, on oral bioavailability and on intestinal secretion of amitriptyline, a tricyclic antidepressant. Amitriptyline was administrated intravenously (5 mg/kg) and orally (50 mg/kg) to rabbits, with and without quinidine. Jejunal segments of rats were mounted on diffusions chambers and the permeation of amitriptyline was measured across the tissue in luminal–serosal (LS) and serosal–luminal (SL) directions, with and without quinidine. Finally, an *in situ* recirculating intestinal perfusion model was performed in rabbits to study amitriptyline permeation in LS direction with and without quinidine. Absolute oral bioavailability (F) of amitriptyline was significantly increased more than three-fold in presence of quinidine ($F = 0.6 \pm 0.4\%$ versus $1.9 \pm 1.1\%$). The apparent permeability coefficients in SL direction were significantly higher than in LS direction ($P_{app\ (SL)} = 6.01 \pm 2.42$ versus $P_{app\ (LS)} = 4.90 \pm 2.73 \times 10^{-4}$ cm min^{-1}). In presence of quinidine, the intestinal absorption was increased ($P_{app\ (LS)} = 4.02 \pm 2.91$ versus $P_{app\ (LS)} = 5.99 \pm 2.43 \times 10^{-4}$ cm min^{-1}) and the intestinal secretion was decreased ($P_{app\ (SL)} = 4.58 \pm 0.54$ versus $P_{app\ (LS)} = 3.63 \pm 1.46 \times 10^{-4}$ cm min^{-1}) but not significantly. In conclusion, P-glycoprotein appears to be involved in oral amitriptyline absorption but other intestinal uptake and efflux transporters maybe implicated.

Keywords: Amitriptyline; Quinidine; P-glycoprotein; Oral bioavailability; Intestinal secretion

1. Introduction

Amitriptyline (AMI) is a tricyclic antidepressant which remains one of the major antidepressants despite the introduction of newer drugs such as selective serotonin reuptake inhibitors (Barbui and Hotopf, 2001). AMI has also analgesic properties and is commonly used in the treatment of chronic pain where it is still the mainstay of front-line therapy of diabetic neuropathy, postherpetic neuralgia, fibromyalgia, central pain and peripheral neuropathy of different etiology (Bryson and Wilde, 1996). The oral bioavailability of AMI is highly variable, ranging from 33 to 62% in humans (Schultz et al., 1985), and is responsible for large interindividual variations in the systemic concentrations and in the therapeutic effects. AMI has been shown to be a substrate of P-glycoprotein (P-gp) in *ex vivo* models (Fardel et al., 1992, Varga et al., 1996) and now, it is widely recognized that P-gp is a major determinant for low and variable oral bioavailability by increasing the exposure of the drug to intestinal cytochrome P450 by allowing repeated cycling of the drug via diffusion and active efflux (Benet et al., 1996; Benet and Cummins, 2001; Wacher et al., 2001). P-gp is a 170-kDa transmembrane protein member of the ATP-binding cassette (ABC) family of transporters acting as an extrusion pump, is considered to be one of the most important factors involved in the multidrug resistance (MDR) to cancer chemotherapy, by leading to the efflux of anticancer drugs from tumor cells (Harris and Hochhauser, 1992). P-gp, originally identified in tumor cells, is also present in normal tissues, particularly in organs where P-gp plays a role in defense against xenobiotics; the protein is found in the biliary canalicular membrane of hepatocytes, in the apical membrane of the intestinal epithelium, in the luminal membrane of proximal tubular epithelial cell of kidneys and in the small blood capillaries of the blood–brain barrier and blood–testis barrier and in placenta (Thiebaut et al., 1987). P-gp is encoded by the ABCB1 (formerly called MDR1) gene in humans and by the abcb1a and abcb1b (formerly called mdr1a and mdr1b) genes in rodents (Gottesman et al., 1995). The range of substrates transported by P-gp is broad including a variety of drugs (Marzolini

* Corresponding author. Tel.: +33 2 23 23 48 72; fax: +33 2 23 23 48 46.
E-mail address: pascal.le-corre@univ-rennes1.fr (P. Le Corre).

0378-5173/$ – see front matter © 2006 Elsevier B.V. All rights reserved.
doi:10.1016/j.ijpharm.2006.09.026

et al., 2004) such as anti-cancer agents (vinblastine, vincristine, doxorubicine), antihypertensive agents (digoxine, quinidine), immunosuppressants (cyclosporine, valspodar), antidepressants (paroxetine, sertraline).

AMI is known to be a substrate of P-gp in *ex vivo* models but also in *in vivo* models where Uhr et al. (2000) showed that central nervous system concentrations of AMI and its metabolites in knockout mice lacking a functional P-gp were higher than in control mice after a single intraperitoneal administration of AMI. Since saturation of P-gp may occur, Grauer and Uhr (2004) investigated whether a significant difference of the cerebral concentrations of AMI and its metabolites between wild and knockout mice was still observed after a repeated administration of AMI. They showed that the cerebral concentrations were significantly increased in the P-gp knockout mice for all metabolites except for AMI and they suggested that this phenomenon could be explained by a changed permeability of the blood–brain barrier for AMI but not for its metabolites. Finally, they compared the pharmacokinetics and metabolism of AMI in knock-out mice and in controls (Uhr et al., 2005). They showed that AMI was similarly metabolized and that there were no significant differences in the pharmacokinetics of AMI in knock-out and in control mice.

Since AMI is mainly administrated via the oral route but also intravenously in acute periods and, since P-gp is located in the enterocytes, it is of interest to evaluate the impact of P-gp on AMI bioavailability following oral dosing. Indeed, P-gp may influence the plasma levels of AMI and therefore the brain levels. Hence, to evaluate the impact of P-gp on AMI bioavailability, we investigated *in vivo* the effect of oral quinidine, a P-gp inhibitor (Ford and Hait, 1990), on pharmacokinetics of AMI after intravenous and oral administration in rabbits. Then, to better understand the influence of quinidine on the intestinal absorption and secretion of AMI, we used an *ex vivo* model of Ussing-type chambers in rats and an *in situ* recirculating intestinal perfusion model in rabbits.

2. Materials and methods

2.1. Chemicals

Amitriptyline hydrochloride, quinidine sulfate dihydrate and clomipramine hydrochloride, used as internal standard, were purchased from Sigma Chemical Co (St. Louis, USA). Amitriptyline metabolites (nortriptyline, *E*- and *Z*-hydroxy-amitriptyline, *E*- and *Z*-hydroxy-nortriptyline) were kindly given by Lundbeck (Copenhagen, Denmark). All other reagents were of analytical or HPLC grade.

2.2. Animals

The study was approved by the Committee of Laboratory Investigation and Animal Care of our institution and performed in accordance with French Ministry of Agricultures laws and guidelines for laboratory animal experiments (agreement no. B35-238-21). Two animal species were used for the study:

- *in vivo* experiments and *in situ* recirculating intestinal perfusion model were performed on New Zealand white adult female rabbits (2.45–3.65 kg) because iterative blood sampling every week during 4 weeks was more technically feasible in rabbits.
- *ex vivo* model of Ussing-type chambers was performed on male Sprague–Dawley rats (350–400 g) because previous experiments in rabbits showed that duodenum and jejunum sections were too thick for diffusion chambers and leaks were observed.

The animals were housed individually and maintained in animal care facilities for at least 1 week before use. They received food and water *ad libitum* and were fasted 12 h before each experiment.

2.3. Study design

The *in vivo* experiment was carried out on six rabbits during 4 weeks. The first week, they received a bolus intravenous administration of AMI (5 mg/kg), the second week a *per os* administration of AMI (50 mg/kg), the third a bolus intravenous administration of AMI (5 mg/kg) with oral QUI (20 mg/kg) 1 h before and finally the fourth week a *per os* administration of AMI (50 mg/kg) with oral QUI (20 mg/kg) 1 h before. Each administration of AMI was separated by a 1 week wash-out period. Blood samples (2 ml) were collected at predetermined times: 0, 2, 5, 10, 20, 30, 45, 60, 90, 120, 240 and 480 min for intravenous AMI administration (with and without QUI) and 0, 10, 20, 30, 45, 60, 90, 120, 240, 360 and 480 min for oral AMI administration (with and without QUI). Plasma was separated from whole blood by centrifugation (3500 × *g* for 10 min) and stored at −20 °C until analysis by HPLC.

The *ex vivo* model of Ussing-type chambers was carried out on seven rats. They were anesthetized with a 50 mg/ml pentobarbital Penthotal® (Abbott, Rungis, France) and 50 mg/ml Ketamine® (Virbac, Carros, France) solution at a dose of 1 ml/kg by subcutaneous injection. The rats were placed on a heating pad to maintain a normal body temperature of 37 °C throughout the experiment. A mid-ventral incision extending 5 cm was made along the *linea alba* and the small intestine was exposed. A cut was made at the junction between the duodenum and the jejunum and a section of small intestine, approximately 30 cm, was removed. The intestinal section was washed with 20 ml of ice cold Krebs's solution (pH 6.5) containing 7 g/l NaCl, 0.34 g/l KCl, 1.8 g/l D-glucose, 0.251 g/l Na_2HPO_4, 0.207 g/l NaH_2PO_4 and 46.8 mg/ml $MgCl_2$. Then, eight sections of about 3 cm length, with no Peyer's patches, were isolated from this intestinal segment, opened along the mesenteric border and immediately mounted in Ussing type chambers (Navicyte, Sparks, USA). The serosal (S) i.e. basolateral side and luminal (L) i.e. brush border or apical side were filled with 8 ml of warm Krebs's solution gassed with 95% O_2 and 5% CO_2. The Ussing type chambers were placed in a temperature-controlled box at 37 °C. AMI used at two concentrations (0.02 or 2 mM) was added to the donor side. The concentration of AMI in the receiver chamber was determined by HPLC and the cumulative amount of

AMI permeating the membrane was calculated based on the chamber volume. Samples were collected in 100 μl aliquots (followed by replacement with buffer) every 15 min for 240 min. QUI (0.2 mM) was added at 150 min to both sides and apparent permeability coefficients (P_{app}) were compared between 60–150 min (without QUI) versus 180–240 min (with QUI). Studies were conducted in both the luminal–serosal (LS) and serosal–luminal (SL) directions.

The *in situ* recirculating intestinal perfusion model was carried out on 10 rabbits. They were anesthetized with a 1% pentobarbital Penthotal® (Abbott, Rungis, France) solution at a dose of 1 ml/kg by intravenous injection. The rabbits were placed on a heating pad to maintain a normal body temperature of 37 °C throughout the experiment. A mid-ventral incision extending 5 cm was made along the *linea alba* and the small intestine was exposed. Approximately, 15 cm of jejunum was externalized and incisions were made at both ends of the jejunal segment. The segment was gently flushed with warm Krebs's solution to remove intestinal contents, cannulated with sections of Silicone tubing at each end and covered by saline-soaked gauze. The inlet jejunal cannula was connected to a peristaltic pump (Ismatec, Glattbrugg, Switzerland) and Krebs's solution was passed through the lumen at 1 ml/min from a jacketed reservoir that maintained the perfusate at 37 °C. The preparation was allowed to stabilize for 30 min, during which time the perfusate exiting the jejunal segment was discarded to waste. After the stabilization period, the perfusate reservoir was replaced with a reservoir containing a precise volume (30 ml) of 2 mM AMI without or with 0.2 mM QUI. After the first minute of perfusion, sufficient to flush the buffer from the system, the outlet cannula was directed to the reservoir to start the recirculation of AMI perfusate. One hundred microliters samples were collected every 10 min for 1 h and immediately analyzed by HPLC.

2.4. Extraction procedure

After thawing, the plasma samples (1 ml) were homogenized and 100 μl of clomipramine (10 μg/ml) used as internal standard, were added. A total of 100 μl of 1N NaOH and 4 ml of heptane with ethyl acetate (80/20) were added and the samples were mixed for 10 min at room temperature. After centrifugation for 5 min at 4000 × *g*, the organic layer was transferred to a tube containing 50 μl of 0.05 M sulfuric acid, mixed for 10 min and centrifuged at 3000 × *g* for 5 min. The organic layer was then discarded and a 50 μl aliquot of the aqueous phase was mixed to 10 μl of 0.5 M dipotassium hydrogen phosphate. Finally 20 μl of the aqueous phase were injected for chromatographic separation. The separation and quantification of AMI and its metabolites in plasma samples were carried out using a HPLC method with UV absorbance detection (λ = 205 nm). The chromatographic system consisted of a Waters model 600A pump (Waters, Milford, USA) equipped with a Waters model 717 automatic injector, a Waters model 996 photodiode array detector and a Waters model Empower integration software. The analytical chromatographic column was a Supelco 5 μm C18 250 mm × 4.6 mm (Sigma–Aldrich, Bellefont, USA) maintained at 45 °C and the flow rate of the mobile phase was 1 ml/min.

The mobile phase A (acetonitrile-water 10/90, 900 μl of 85% phosphoric acid, 1.22 g of potassium dihydrogen phosphate) and B (acetonitrile) were filtered through a 0.45 μm PTFE membrane (Millipore, St. Quentin, France) and degassed immediately before use. A 20–50% mobile phase B gradient in 21 min was used for chromatographic analysis. Plasma samples were calibrated by using seven different concentrations ranging from 5 to 1000 ng/ml. Quantification was performed by calculating the analyte/internal standard peak–area ratio.

2.5. Pharmacokinetic analysis

Pharmacokinetic parameters were determined by using a bicompartmental model after IV administration and a noncompartmental analysis after oral administration with the software package WinNonlin (version 4-0; Scientific Consulting Inc, Apex, USA). The area under the plasma concentration–time curves (AUC) were calculated by trapezoidal rule. The clearance was calculated by dose/AUC. The apparent elimination half-life ($t_{1/2}$) was obtained by $0.693/k_{el}$ where k_{el} is the elimination rate constant. The first-order elimination (k_{10}) and distribution (k_{12} and k_{21}) microconstants were calculated. The maximum plasma concentration (C_{max}) and the time to reach the maximum plasma concentration (T_{max}) were obtained from experimental data.

Finally, the oral bioavailability (F) of AMI was calculated: $F = (AUC_{oral}/AUC_{IV} \times \text{IV dose/oral dose}) \times 100$.

Apparent permeability coefficients (P_{app}) in the *ex vivo* model of Ussing-type chambers were calculated by the equation:

$$P_{app}\,(\text{cm min}^{-1}) = \frac{dQ/dt}{AC_0}$$

where dQ/dt is the rate of AMI appearance in the receiver side (μmol min^{-1}), A the effective surface area available for diffusion ($A = 1.78$ cm^2) and C_0 is the concentration of AMI in the donor side at initial time t_0.

In the *in situ* recirculating intestinal perfusion model, P_{app} of AMI was calculated from its disappearance from the luminal perfusate where dQ/dt is the rate of AMI disappearance from perfusate (μmol min^{-1}), A the measured surface area of the jejunal segment (cm^2) and C_0 is the concentration of AMI in the perfusate at initial time t_0.

2.6. Statistical analysis

All data are presented as mean ± S.D. Student's t test was used to compare individual parameters, and diffusion studies were analyzed using an analysis of variance followed by multiple comparison testing. A p-value less than 0.05 was considered as statistically significant.

3. Results

3.1. Pharmacokinetic analysis

Plasma AMI concentration–time curves after IV administration with and without QUI are shown in Fig. 1a and AMI pharmacokinetic parameters are presented in Table 1. There was

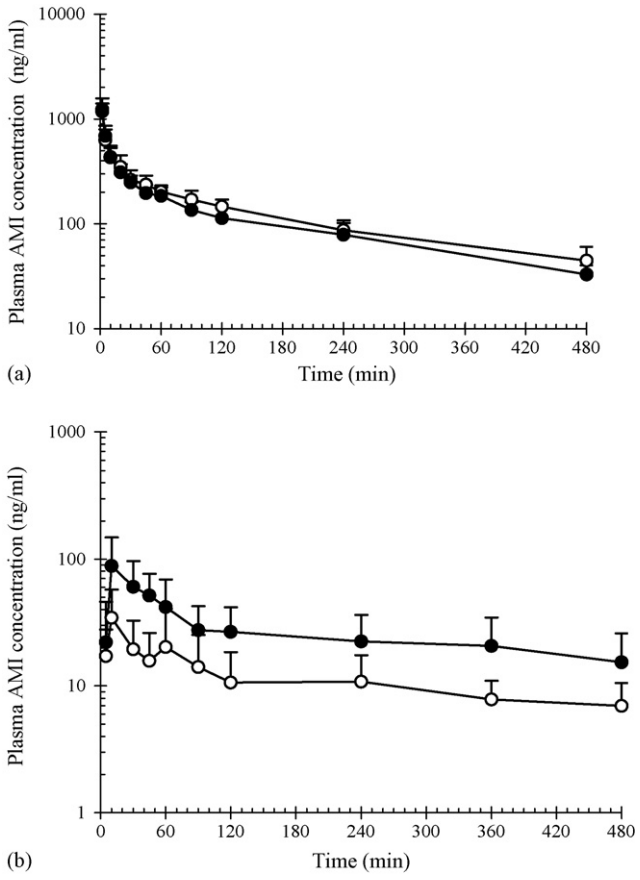

Fig. 1. Plasma amitriptyline concentration–time profile after IV administration (a) and after oral administration (b) without (open circles) and with quinidine (closed circles) in rabbits. Each point represents the mean ± S.D. ($n = 6$).

significant difference neither in pharmacokinetic parameters of AMI (Table 1) nor in plasma AMI concentrations (Fig. 1a) after IV administration with QUI pretreatment.

Plasma AMI concentration–time curves after oral administration with and without QUI are shown in Fig. 1b and the AMI parameters in Table 2. With QUI pretreatment, AUC and C_{max} increased significantly two-fold after AMI oral administration while $t_{1/2}$ was unchanged (Table 2 and Fig. 1b).

The influence of QUI on AMI bioavailability (F) is shown in Table 3. In presence of QUI, F increased significantly more than three-fold (0.6 ± 0.4% versus 1.9 ± 1.1%).

Table 1
Pharmacokinetic parameters of amitriptyline after IV administration with and without quinidine in rabbits ($n = 6$)

	Q(−)[a]	Q(+)[b]
AUC (ng ml^{-1} min)	76568 ± 10555	66603 ± 15291
$t_{1/2}$ (min)	174 ± 30	166 ± 23
CL (ml min^{-1} kg^{-1})	66 ± 9	78 ± 17
Vss (l)	14 ± 4	14 ± 5
k_{10} (h^{-1})	0.014 ± 0.004	0.014 ± 0.005
k_{12} (h^{-1})	0.350 ± 0.165	0.269 ± 0.165
k_{21} (h^{-1})	0.079 ± 0.05	0.090 ± 0.064

Values are mean ± S.D.
[a] Q(−) without quinidine.
[b] Q(+) with quinidine.

Table 2
Pharmacokinetic parameters of amitriptyline after oral administration with and without quinidine in rabbits ($n = 6$)

	Q(−)[a]	Q(+)[b]
AUC (ng ml^{-1} min)	4782 ± 3077	11053 ± 5814*
$t_{1/2}$ (min)	505 ± 181	490 ± 297
T_{max} (min)	20 ± 19	40 ± 12
C_{max} (ng ml^{-1})	33 ± 16	69 ± 43*

Values are mean ± S.D.
* Significant difference.
[a] Q(−) without quinidine.
[b] Q(+) with quinidine.

The contribution of AMI metabolites after IV and oral administration with and without QUI is presented in Table 4. After IV administration, only NOR, *E*- and *Z*-OH-AMI were detected and plasma metabolites AUC were not influenced by QUI. After oral administration, AUC of NOR increased about six-fold, *E*-OH-NOR four-fold ($p < 0.05$), *E*-OH-AMI and *Z*-OH-NOR two-fold and *Z*-OH-AMI 1.5-fold in presence of QUI.

3.2. Ex vivo model of Ussing-type chambers

This *ex vivo* model has been used to determine if an intestinal secretion occurs.

A comparison of the AMI permeation coefficients across rat jejunum in the LS and SL directions without QUI is given in Table 5. At two concentrations of AMI, the apparent permeability coefficient (P_{app}) of AMI in the SL direction was significantly higher than in the LS direction, which suggests that AMI is secreted.

To analyze the influence of a P-gp inhibitor on AMI secretion and absorption, permeation rates of AMI in the LS and SL directions were compared with and without QUI (Tables 6 and 7).

At 0.02 mM AMI, P_{app} in LS direction was increased approximately by 50% after pretreatment by QUI but not significantly and at 2 mM AMI, P_{app} in LS direction was not influenced by QUI.

At 0.02 mM AMI, P_{app} in SL direction was decreased approximately by 20% after pretreatment by QUI, but not significantly while at 2 mM AMI, P_{app} was significantly increased.

3.3. In situ recirculating intestinal perfusion model

To confirm the role of QUI on the intestinal transport and uptake of AMI, we used the *in situ* recirculating intesti-

Table 3
Influence of quinidine on bioavailability of amitriptyline in rabbits ($n = 6$)

	F (%)
Q(−)[a]	0.6 ± 0.4
Q(+)[b]	1.9 ± 1.1*

Values are mean ± S.D.
* Significant difference.
[a] Q(−) without quinidine.
[b] Q(+) with quinidine.

Table 4
Plasma metabolites AUC (ng ml^{-1} min) after IV and oral administration with and without quinidine in rabbits ($n = 6$)

	IV		Oral	
	Q(−)[a]	Q(+)[b]	Q(−)[a]	Q(+)[b]
NOR	1263 ± 512	1908 ± 583	2699 ± 1298	15558 ± 14830
E-OH-AMI	1851 ± 1151	2892 ± 3861	4651 ± 2976	10025 ± 4932
E-OH-NOR	–	–	3554 ± 1991	14248 ± 6061*
Z-OH-AMI	1295 ± 1046	1769 ± 925	1371 ± 200	2144 ± 617
Z-OH-NOR	–	–	1027 ± 147	1844 ± 602

Values are mean ± S.D. NOR: Nortriptyline; *E*-OH-AMI: *E*-OH-Amitriptyline; *E*-OH-NOR: *E*-OH-Nortriptyline; *Z*-OH-AMI: *Z*-OH-Amitriptyline; *Z*-OH-NOR: *Z*-OH-Nortriptyline.
* Significant difference.
[a] Q(−) without quinidine.
[b] Q(+) with quinidine.

Table 5
Apparent permeability coefficients of amitriptyline in LS and SL directions without quinidine in rats ($n = 7$)

	P_{app} LS ($\times 10^4$ cm min^{-1})	P_{app} SL ($\times 10^4$ cm min^{-1})
AMI (0.02 mM)	4.90 ± 2.73	6.01 ± 2.42*
AMI (2 mM)	3.80 ± 0.06	4.44 ± 0.60*

Values are mean ± SD.
* Significant difference.

Table 6
Influence of quinidine on apparent permeability coefficients of amitriptyline in LS direction in rats ($n = 7$)

	P_{app} LS Q(−)[a] ($\times 10^4$ cm min^{-1})	P_{app} LS Q(+)[b] ($\times 10^4$ cm min^{-1})
AMI (0.02 mM)	4.02 ± 2.91	5.99 ± 2.43
AMI (2 mM)	3.58 ± 0.71	3.22 ± 1.06

Values are mean ± S.D.
[a] Q(−) without quinidine.
[b] Q(+) with quinidine.

nal perfusion model which evaluates the transport in the LS direction.

The influence of QUI on the disappearance of AMI from the luminal perfusate is shown in Fig. 2. Apparent permeability coefficients ($\times 10^4$ cm min^{-1}) of AMI were P_{app} LS = 5.33 ± 0.95 without QUI and P_{app} LS = 6.80 ± 1.34 with QUI. Thus, the transport in the LS direction was increased approximately by 30% with QUI pretreatment, although this difference was not significant.

Table 7
Influence of quinidine on apparent permeability coefficients of amitriptyline in SL direction in rats ($n = 7$)

	P_{app} SL Q(−)[a] ($\times 10^4$ cm min^{-1})	P_{app} SL Q(+)[b] ($\times 10^4$ cm min^{-1})
AMI (0.02 mM)	4.58 ± 0.54	3.63 ± 1.46
AMI (2 mM)	4.95 ± 1.78	7.69 ± 1.60*

Values are mean ± S.D.
* Significant difference.
[a] Q(−) without quinidine.
[b] Q(+) with quinidine.

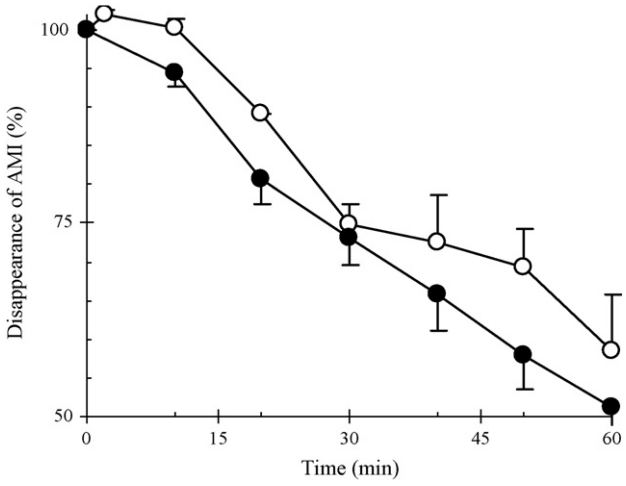

Fig. 2. Disappearance of amitriptyline from the luminal perfusate (%) without (open circles) and with quinidine (closed circles) in rabbits. Each point represents the mean ± S.D. ($n = 10$).

4. Discussion

Amitriptyline is known to belong to Class 1 of the biopharmaceutics classification system (BCS) where compounds are characterized by a high solubility and a high permeability. Wu and Benet (2005) suggested that a modified version of this classification, the biopharmaceutics drug disposition classification system (BDDCS) may be useful in predicting overall drug disposition and effects of efflux and absorptive transporters on oral drug absorption. Based on the BDDCS, AMI was expected to have a low bioavailability and to be minimally affected by transport effects.

In vivo experiments showed that bioavailability of AMI was very low and increased significantly more than three-fold ($p < 0.05$) in presence of QUI (Table 3). Increased bioavailability of a drug in presence of QUI was already observed. Sadeque et al. (2000) showed that the co-administration in healthy volunteers of 600 mg QUI with a 16 mg dose of loperamide increased AUC of loperamide compared with placebo (AUC = 99.5 ± 20.3 versus 247.5 ± 45.2 ng/ml h). Kharasch et al. (2004) also showed that QUI pretreatment (600 mg) with oral

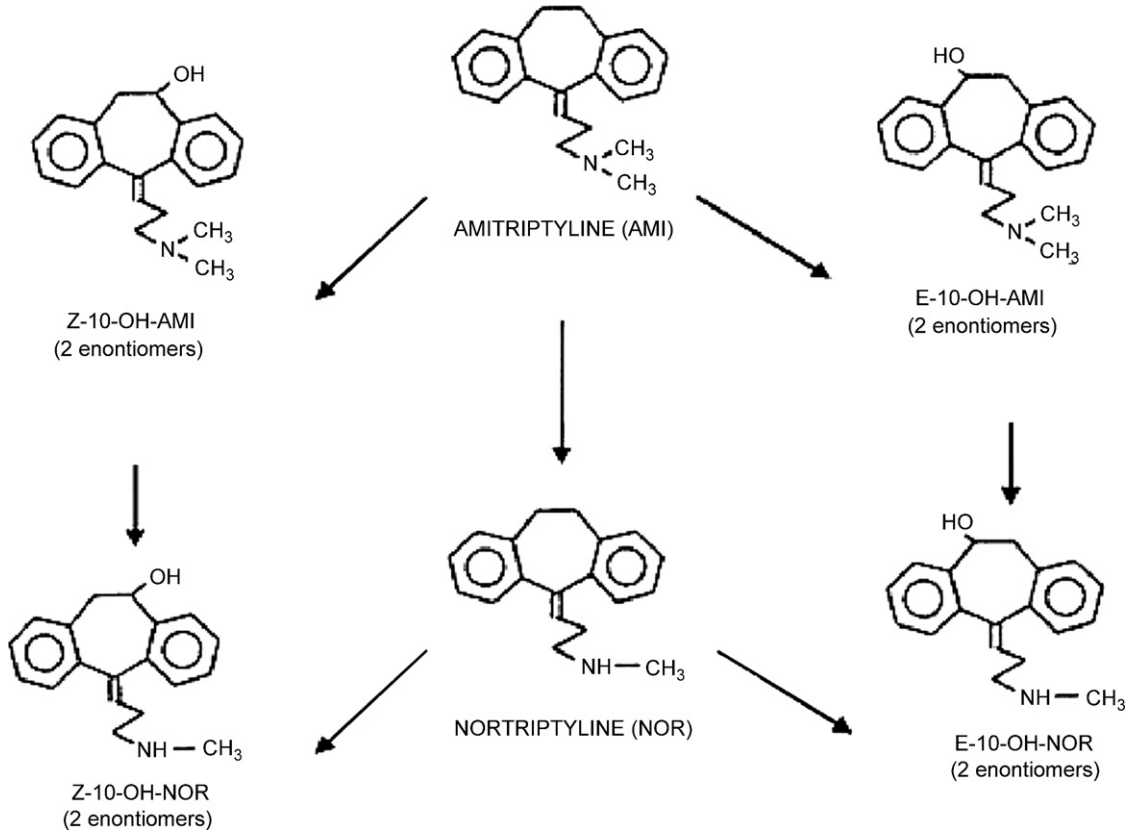

Fig. 3. Main metabolic pathways of amitriptyline metabolism in rabbits.

administration of fentanyl (2.5 μg/kg) increased plasma C_{max} (0.21 ± 0.10 versus 0.55 ± 0.16 ng/ml) and AUC (0.7 ± 0.3 versus 1.9 ± 0.5 ng/ml h). QUI is known to be an inhibitor of CYP2D6, and in vitro and *in vivo* studies in humans have shown that CYP2D6 is the major determinant of the hydroxylation leading to *E*/*Z*-OHAMI and *E*/*Z*-OHNOR (Venkatakrishnan et al., 2001). Main metabolic pathways of AMI metabolism in rabbits are shown in Fig. 3. The inhibition of CYP2D6 by QUI may be a confounding factor that led to an increase of bioavailability of AMI by inhibiting AMI metabolism. However, after QUI administration, we observed increased plasma concentrations of hydroxylated metabolites: AUC of *E*-OH-NOR was increased about fourfold, *E*-OH-AMI and *Z*-OH-NOR two-fold and *Z*-OH-AMI 1.5-fold (Table 4). Moreover, we observed an increase in AUC of NOR of about six-fold. Such an increase may be explained by the fact that AMI *N*-demethylation leading to NOR is mainly mediated by CYP2C19 but also by CYP3A4 (Venkatakrishnan et al., 1998). CYP2C19 shows high affinity and is dominant at low AMI concentrations (5 μmol l^{-1}), while CYP3A4 shows low affinity and is more important at higher AMI concentrations (100 μmol l^{-1}). Thus, the interplay between P-gp and CYP3A4 may explain this increase in plasma concentrations of NOR because the inhibition of P-gp by QUI may decrease active efflux of AMI and increase the exposure of the AMI to intestinal cytochrome CYP3A4. Hence, these results suggest that the increase of oral AMI bioavailability likely results from the inhibition of the P-glycoprotein-mediated efflux by QUI pretreatment.

To confirm the implication of P-gp in the intestinal secretion of AMI, we used an *ex vivo* model of Ussing-type chambers and an *in situ* recirculating intestinal perfusion model. As shown in Table 5, P_{app} of AMI in the SL direction was significantly higher than in the LS direction which suggests that AMI is secreted. Then, to evaluate the influence of QUI on the intestinal absorption and secretion of AMI, we studied LS and SL transport with and without QUI. In presence of QUI, LS transport at 0.02 mM AMI was increased approximately by 50% (Table 6) and, in the recirculating intestinal perfusion model, the apparent permeability coefficient of AMI was increased approximately by 30% (Fig. 2). Such a model has already been used to study the influence of QUI on drug transport. Su and Huang (1995) showed in the model of ileal everted sacs that QUI increased significantly the appearance of digoxine in the serosal side by two-fold. Indeed, QUI by inhibiting P-gp increased net AMI intestinal absorption. Thus, the implication of P-gp in intestinal transport of AMI was in accordance with Uhr who showed that AMI was substrate of P-gp. However, the influence of QUI on the SL transport of AMI showed unexpected results. At 0.02 mM AMI, P_{app} in SL direction was decreased approximately by 20% after pretreatment by QUI; this result was expected because QUI by inhibiting P-gp led to a decrease of active efflux. But, in contrast, one unexpected finding is that at 2 mM AMI, P_{app} in SL direction was increased in presence of QUI (Table 7).

An assumption for this unexpected result is that P-gp, which is a saturable transporter, may be saturated by a too large AMI concentration. This hypothesis is supported by the fact that at 2 mM AMI, P_{app} in LS direction was not influenced by QUI (Table 6) and was increased in SL direction (Table 7) whereas an increase of absorption and a decrease of secretion were expected in presence of QUI.

An other explanation may be that AMI transport could involve other intestinal transporters, such as other members of ABC transporters like the MRP (multidrug resistance-associated protein) subfamily or members of organic cation transporter (OCT) and organic anion-transporting polypeptide (OATP) families. Active efflux transporters such as Mrp2 are localized on the apical brush-border membrane of the villus tip enterocytes where they efflux their substrates into the lumen resulting in a potential limitation of net absorption. However some ABC transporters such as Mrp1 and Mrp3 are localized to the basolateral membranes of intestinal polarized epithelial cells in small intestine and colon (Peng et al., 1999; Kiuchi et al., 1998) where they mediate the transport of drugs in the opposite direction. Other transporters such as members of the organic cation transporter (OCT) family are expressed on basolateral membrane. In rats, Oct1 is predominantly localized in the basolateral membrane of hepatocytes and intestinal epithelial cells and mediates the uptake of several substrate drugs such as QUI (Arndt et al., 2001; Van Montfoort et al., 2001) and desipramine and imipramine, tricyclic antidepressants with a very close chemical structure to that of AMI (Arndt et al., 2001; Wu et al., 2000). Therefore it would be possible for AMI to be an Oct1 substrate and the inhibition of Oct1 by QUI pretreatment would lead to a decrease of intestinal absorption and increase of intestinal secretion of AMI.

In conclusion, this study showed that quinidine increased significantly the absolute oral bioavailability of amitriptyline, suggesting the involvement of P-glycoprotein in amitriptyline disposition. However, unexpected findings in *ex vivo* and *in situ* experiments led us to assume that quinidine may inhibit other intestinal transporters and that P-gp may not be a major player in the oral bioavailability and intestinal secretion of amitriptyline. Hence, to better delineate the disposition of this widely used drug, further studies are needed on the putative transporters involved in the oral bioavailability of amitriptyline and on its distribution in P-gp expressing organs (e.g., liver) implicated in its disposition.

Acknowledgement

We are grateful to Lundbeck Company (Copenhagen, Denmark) which kindly supplied us with amitriptyline metabolites.

References

Arndt, P., Volk, C., Gorboulev, V., Budiman, T., Popp, C., Ulzheimer-Teuber, I., Akhoundova, A., Koppatz, S., Bamberg, E., Nagel, G., Koepsell, H., 2001. Interaction of cations, anions and weak base quinine with rat renal cation transporter rOCT2 compared with rOCT1. Am. J. Physiol. Renal Physiol. 281, F454–F468.

Barbui, C., Hotopf, M., 2001. Amitriptyline vs. the rest: still the leading antidepressant after 40 years of randomized controlled trials. Br. J. Psychiatry 178, 129–144.

Benet, L.Z., Wu, C.Y., Hebert, M.F., Wacher, V.J., 1996. Intestinal drug metabolism and antitransport processes: a potential paradigm shift in oral drug delivery. J. Control. Release 39, 139–143.

Benet, L.Z., Cummins, C.L., 2001. The drug efflux-metabolism alliance: biochemical aspects. Adv. Drug Deliv. Rev. 50, S3–S11.

Bryson, H.M., Wilde, M.I., 1996. Amitriptyline: a review of its pharmacological properties and therapeutic use in chronic pain states. Drugs and aging 8, 459–476.

Fardel, O., Ratanasavanh, D., Loyer, P., Ketterer, B., Guillouzo, A., 1992. Overexpression of the multidrug resistance gene product in adult rat hepatocytes during primary culture. Eur. J. Biochem. 205, 847–852.

Ford, J.M., Hait, W.N., 1990. Pharmacology of drugs that alter multidrug resistance in cancer. Pharmacol. Rev. 42, 155–199.

Gottesman, M.M., Hrycyna, C.A., Schoenlein, P.V., Germann, U.A., Pastan, I., 1995. Genetic analysis of the multidrug transporter. Annu. Rev. Genet. 29, 607–649.

Grauer, T.M., Uhr, M., 2004. P-glycoprotein reduces the ability of amitriptyline metabolites to cross the blood–brain barrier in mice after a 10-day administration of amitriptyline. J. Psychopharmacol. 18, 66–74.

Harris, A.L., Hochhauser, D., 1992. Mechanisms of multidrug resistance in cancer treatment. Acta Oncol. 31, 205–213.

Kharasch, E.D., Hoffer, C., Altuntas, T.G., Whittington, D., 2004. Quinidine as a probe for the role of P-glycoprotein in the intestinal absorption and clinical effects of fentantyl. J. Clin. Pharmacol. 44, 224–233.

Kiuchi, Y., Suzuki, H., Hirohashi, T., Tyson, C.A., Sugiyama, Y., 1998. cDNA cloning and inducible expression of human multidrug resistance associated protein 3 (MRP3). FEBS Lett. 433, 149–152.

Marzolini, C., Paus, E., Buclin, T., Kim, R.B., 2004. Polymorphisms in human MDR1 P-glycoprotein: recent advances and clinical relevance. Clin. Pharmacol. Ther. 75, 13–33.

Peng, K.C., Cluzeaud, F., Bens, M., Duong Van Huyen, J.P., Wioland, M.A., Lacave, R., Vandewalle, A., 1999. Tissue and cell distribution of the multidrug resistance-associated protein (MRP) in mouse intestine and kidney. J. Histochem. Cytochem. 47, 757–768.

Sadeque, A.J.M., Wandel, C., He, H., Shah, S., Wood, A.J.J., 2000. Increased drug delivery to the brain by P-glycoprotein inhibition. Clin. Pharmacol. Ther. 68, 231–237.

Schultz, P., Dick, P., Blaschkle, T.F., Hollister, L., 1985. Discrepancies between pharmacokinetic studies of amitriptyline. Clin. Pharmacokinet. 10, 257–268.

Su, S.F., Huang, J.D., 1995. Inhibition of the intestinal digoxin absorption and exsorption by quinidine. Drug Metabol. Dispos. 24, 142–147.

Thiebaut, F., Tsuruo, T., Hamada, H., Gottesman, M.M., Pastan, I., Willingham, M.C., 1987. Cellular localization of the multidrug-resistance gene product P-glycoprotein in normal human tissues. Proc. Natl. Acad. Sci. USA 84, 7735–7738.

Uhr, M., Steckler, T., Yassouridis, A., Holsboer, F., 2000. Penetration of amitriptyline, but not fluoxetine into brain is enhanced in mice with blood–brain barrier deficiency due to mdr1a P-glycoprotein gene disruption. Neuropsychopharmacology 22, 380–387.

Uhr, M., Grauer, M.T., Yassouridis, A., Ebinger, M., 2005. Blood–brain barrier penetration and pharmacokinetics of amitriptyline and its metabolites in P-glycoprotein (abcb 1 ab) knock-out mice and controls. J. Psychiatr. Res., 29.

Van Montfoort, J.E., Muller, M., Groothuis, G.M.M., Meijer, D.K.F., Koepsell, H., Meier, P.J., 2001. Comparison of "type I" and "type II" organic cation transport by organic cation transporters and organic anion-transporting polypeptides. J. Pharmacol. Exp. Ther. 298, 110–115.

Varga, A., Nugel, H., Baerh, R., Marx, U., Hever, A., Nasca, J., Ocsovsky, I., Molnar, J., 1996. Reversal of multidrug resistance by amitriptyline in vitro. Anticancer res. 16, 209–211.

Venkatakrishnan, K., Greenblatt, D.J., Von Molkte, L.L., Schmider, J., Harmatz, J.S., Shader, R.I., 1998. Five distinct human cytochromes mediate amitriptyline *N*-demethylation in vitro: dominance of CYP2C19 and 3A4. J. Clin. Pharmacol. 38, 112–121.

Venkatakrishnan, K., Schmider, J., Harmatz, J.S., Ehrenberg, B.L., Von Molkte, L.L., Graf, J.A., Mertazis, P., Corbett, K.E., Rodriguez, M.C., Shader, R.I., Greenblatt, D.J., 2001. Relative contribution of CYP3A to amitriptyline clearance in humans: in vitro and in vivo studies. J. Clin. Pharmacol. 41, 1043–1054.

Wacher, J.V., Salphati, L., Benet, L.Z., 2001. Active secretion and enterocytic drug metabolism barriers to drug absorption. Adv. Drug Deliv. Rev. 46, 89–102.

Wu, X., George, R.L., Huang, W., Wang, H., Conway, S.J., Leibach, F.H., Ganpathy, V., 2000. Structural and functional characteristics and tissue distribution pattern of rat OCTN1, an organic cation transporter, cloned from placenta. Biochim. Biophys. Acta 1466, 315–327.

Wu, C.Y., Benet, L.Z., 2005. Predicting drug disposition via application of BCS: transport/absorption/elimination interplay and development of a biopharmaceutics drug disposition classification system. Pharm. Res. 22, 11–23.